Supporting Information

Precision Photothermal Therapy and Photoacoustic Imaging by *In Situ* Activatable Thermoplasmonics

Yahua Liu,‡ Fengye Mo,‡ Jialing Hu, Qunying Jiang, Xiuyuan Wang, Zhiqiao Zou, Xian-Zheng Zhang, Dai-Wen Pang, and Xiaoqing Liu*

College of Chemistry and Molecular Sciences, Wuhan University, Wuhan 430072, P. R. China.

* E-mail: xiaoqingliu@whu.edu.cn.

‡ These authors contributed equally to this work

Table of Contents

Supporting Information

Supporting Information

Experimental Section

Materials

Hydrogen tetrachloroauratetrihydrate ($HAuCl_4 \cdot 3H_2O$), sodium citrate, silver nitrate ($AgNO_3$), polyvinylpyrrolidone (PVP, MW = 10000), L-ascorbic acid (AA) and Tween 20 were obtained from Sigma-Aldrich. mPEG-SH (MW = 5000) was purchased from JenKem Technology (China). N-Acetyl-L-Cysteine (NAC) was obtained from Aladdin Reagent (Shanghai, China). Dulbecco's modified eagle's medium (DMEM) was obtained from Gibco. Fetal bovine serum (FBS) was provided by AusGeneX. Paraformaldehyde (4%) was obtained from Boster Biological Technology Co., Ltd. Annexin V-FITC apoptosis detection kit was purchased from Best Bio Science Co., Ltd. The calcein-AM/PI double-stain kit was purchased from Shanghai Yeasen Biotechnology Co., Ltd. Penicillin-streptomycin, trypsin, and 2-(4-Amidinophenyl)-6-indolecarbamidine dihydrochloride (DAPI) were obtained from Beyotime Biotechnology Co., Ltd. All other chemical reagents were of analytical grade. Oligonucleotides were synthesized and HPLC-purified by Sangon Biotech. Co., Ltd. (Shanghai, China), the sequences were listed below (from 5' to 3'):

AS1411: GGT GGT GGT GGT TGT GGT GGT GGT GGT T

SH-AS1411: SH-TTT TTT GGT GGT GGT GGT TGT GGT GGT GGT GGT T

SH-AS1411-TAMRA: SH-TTT TTT GGT GGT GGT GGT TGT GGT GGT GGT GGT T-TAMRA

Characterization

Transmission-electron microscopy (TEM) images were obtained with a JEOL JEM-2100 Plus electron microscope. Ultraviolet-visible (UV-vis) absorption spectra were recorded with a UV-2660 UV-vis spectrophotometer (Shimadzu, Tokyo, Japan). Fluorescent spectra were performed on Cary Eclipse fluorescence spectrophotometer (Agilent Technologies, USA). Dynamic light scattering (DLS) measurements were performed on Nano-ZS90 Zetasizer (Malvern, UK). The content of Au and Ag were determined by contrAA700 inductively coupled plasma atomic absorption spectrometer (ICP-AAS, Analytik Jena AG, Germany) and inductively coupled plasma mass spectroscopy (ICP-MS, Thermo Scientific X series II, USA). The photothermal effect was performed with an 808 nm NIR laser (Hi-Tech Optoelectronics Co., Ltd), and the temperature changes were monitored by a thermocouple microprobe or an IR thermal camera (Fotric, China). Photoacoustic (PA) imaging was recorded with a Vevo LAZR Imaging System (FujiFilm VisualSonic Inc, Canada).

Synthesis of Core-Shell Au@Ag Nanostars

The gold nanostars (AuNS) core were synthesized through a modified method of seed-mediated growth.[1,2] The seed solution was prepared by mixing 4 mL of 1% sodium citrate with 50 mL of 0.5 mM $HAuCl_4$ boiling aqueous solution for 30 min. The as-formed seeds then were functionalized with polyvinylpyrrolidone (PVP) by mixing the seed with PVP under stirring for 24 h at room temperature. Then the mixture was washed three times with ethanol, and dispersed in 5 mL ethanol. To obtain small asymmetric gold nanostars, 82 μL of 50 mM $HAuCl_4$ solution was mixed with 15 mL of 10 mM PVP solution in N, N-Dimethylformamide (DMF), followed by

the rapid addition of the PVP-capped AuNPs solution (43 μL). After stirring 15 min, the color of the solution changed from pink to colorless and finally to blue, confirming the formation of AuNS. After removing excess PVP through washing, $AgNO_3$ and AA were added to synthesize silver shells. 100 μL of 3 mM $AgNO_3$, 100 μL of 40 mM AA, and 200 μL of the obtained AuNS were added into 600 μL of 0.1 M Tris-HCl (pH = 9.5) for 1 h at 37 °C. The as-prepared Au@Ag nanostars were collected by centrifugation at 6000 rpm for 5 min and redispersed in ultrapure water.

Preparation of Au@Ag@PEG/Apt Nanostars

Polyethylene glycol (PEG) was modified on the surface of Au@Ag nanostars to increase its biostability and biocompatibility.[3] Briefly, 10 mM PEG (mPEG-SH, MW = 5000) solution was added to Au@Ag solution for 12 h at 37 °C, and excess PEG was removed by centrifugation (6000 rpm, 5 min). The purified Au@Ag@PEG were redispersed in water.

Thiolated-AS1411 (SH-AS1411) aptamer was further conjugated to Au@Ag@PEG by a freezing-thawing method.[4,5] SH-AS1411 solution (10 mM, 4 μL) was added to the Au@Ag@PEG solution, followed by placing in a freezer (-20 °C) for 2 h. Excess aptamers were removed by centrifugation at 10000 rpm for 5 min after thawing at room temperature. Finally, the prepared Au@Ag@PEG/Apt were dispersed in PBS for further use.

H_2O_2 Activated-Photothermal Effect of Au@Ag@PEG/Apt

Au@Ag@PEG/Apt aqueous solution (28 μg/mL) were mixed with different concentrations H_2O_2 (0, 0.1, 0.5, 1, or 10 mM) for 2 h at 37 °C. Then the solutions were irradiated with a laser

(808 nm, 1W/cm^2) for 10 min, and the temperature was recorded by a thermocouple microprobe or infrared thermal camera. The photothermal stability of Au@Ag@PEG/Apt before or after 100 μM H_2O_2 activation was estimated by constantly subjecting the system first to laser irradiation (808 nm, 1W/cm^2,10 min) and then cooling to room temperature without irradiation for five times.

Cell Culture

Human embryonic kidney transformed cells (HEK-293T), human breast cancer cells (MDA-MB-231), and mouse breast cancer cells (4T1) were cultured in DMEM medium with 10% FBS and 1% antibiotics (penicillin-streptomycin, 10000 U/mL) at 37 °C under a 5% CO_2 humidified atmosphere.

Cellular Uptake Study

MDA-MB-231 cells were seeded in a 6-well plate at a density of 1×10^5 cells per well for 24 h. TAMRA-labeled Au@Ag@PEG/Apt (40 μg/mL) were added to each well and incubated with different time (0, 2, 4, or 8 h). Excess nanoprobes were removed and the cells were washed with PBS for three times. Then, the cells were analyzed by flow cytometry (Beckman Coulter Cyto-FLEX™ (CytoFLEXS)) and confocal microscopy (Revolution XD, Andor, UK).

To investigate the specific targeting property of Au@Ag@PEG/Apt, MDA-MB-231 cells were firstly pretreated with free AS1411. The cancer cells without pre-treatment were used as the control cells. Subsequently, the two group cells were incubated with TAMRA-labeled Au@Ag@PEG/Apt. After 4 h incubation, the cells were analyzed via flow cytometry or spinning-disk confocal microscopy.

Evaluation of Intracellular H_2O_2 Level

Hydrogen peroxide assay kit was utilized to detect the amount of H_2O_2 in MDA-MB-231 cells. NAC (an inhibitor of H_2O_2) and AA (an enhancer of H_2O_2) were respectively incubated with cancer cells for 1 h. Cancer cells alone without treatment were used as control cells. Then the cells were lysed with lysis buffer (RIPA buffer) and centrifuged at 14000 rpm for 10 min. The supernatant was collected for H_2O_2 detection via hydrogen peroxide assay kit according to the manufacturer's instructions (Sangon Biotech).

In Vitro Cytotoxicity Assay

MDA-MB-231, 4T1, and HEK-293T cells (1×10^4 cells per well) seeded into 96-well plates were incubated with Au@Ag@PEG/Apt NS in different concentrations (0, 10, 20, 40, 60, 80, and 100 μg/mL) for 4 h. The cells were washed three times with PBS and fed with fresh medium, followed by irradiating with laser for 10 min (808 nm, 1W/cm^2). After incubating for another 24 h, cell viability was measured with a standard MTT procedure. Absorbance at 490 nm was measured, and the cell viability was calculated according to the manufacturer's instructions.

Live/Dead Cell Staining and Apoptosis Assay

MDA-MB-231 cells (5×10^5 cells per well) were seeded in 35-mm confocal dishes overnight and then incubated with Au@Ag@PEG/Apt or Au@Ag@PEG, separately. After incubation for 4 h and washing with PBS for three times, the cells were fed with fresh medium and irradiated with 808 nm laser for 10 min at a power density of 1 W/cm^2. The cells without treatment were used as the control cells. The cells were subsequently incubated overnight and stained with calcein-AM

(4 μM) and PI (2 μM) for 15 min. Finally, the cells were washed with PBS and imaged by a spinning-disk confocal microscopy. For cell apoptosis analysis, the cells were stained with Annexin V-FITC/PI and then analyzed with flow cytometer.

Establishment of Tumor Models

All animal procedures were in accordance with the National Institute of Health Guide for the Care and Use of Laboratory Animals and approved by Use Committee of the Animal Experiment Center/Animal Biosafety Level-III Laboratory of Wuhan University (license number: WP2020-08047). Female BALB/c mice (5-6 weeks, ~20 g) were purchased from the Laboratory Animal Center of Hubei province and fed under normal conditions with free access to food and water. 4T1 tumor-bearing mice models were established by subcutaneously injecting a suspension of 4T1 cells (1×10^6 cells per mouse, 50 μL in PBS) into the selected positions of the mice. The tumors grow to ~100 mm^3 before treatment.

Pharmacokinetics and Biodistribution

BALB/c mice were intravenously injected with Au@Ag@PEG/Apt NS (500 μg/mL, 60 μL). Blood samples (10 μL) of the mice were subsequently collected at different post-injection time (0.25, 0.5, 1, 2, 3, 4, 8, 12, and 24 h) and dissolved in aqua regia (HCl: HNO_3 = 3:1) for ICP-MS analysis. To study the biodistribution of Au@Ag@PEG/Apt, the mice were sacrificed after 24 h intravenous injection. Tumors and five major organs (heart, liver, spleen, lung, and kidney) were harvested and digested by aqua regia for Au content analysis.

***In Vivo* Photoacoustic Imaging**

Au@Ag@PEG/Apt (500 μg/mL, 100 μL) were intravenously injected into tumor-bearing mice. The photoacoustic images were obtained at 0, 4, 8, and 24 h, respectively via a Vevo LAZR imaging system. NAC (100 mM, 25 μL) was intratumorally administered to each mouse. PBS-treated mice were used as control. After 12 h post-injection, Au@Ag@PEG/Apt was subsequently intratumorally injected. The photoacoustic images of different treatment-mice were acquired at different time (0, 0.5, 4, and 8 h) via a Vevo LAZR imaging system.

For lymph node metastasis imaging, 4T1 cells (1×10^6 cells per mouse, 20 μL in PBS) were injected into the right hind footpad of mice. After 19 days, mice with spherical firm lumps touchable in their inner knees were chosen for PA imaging. Au@Ag@PEG/Apt was subcutaneously injected into the interstitial space between the primary tumors and the metastatic lymph nodes. Contralateral normal lymph nodes were regarded as the control and injected with the same amount of nanoagents. The photoacoustic images of lymph nodes were acquired at different time points after injection.

***In Vivo* Photothermal Imaging**

Au@Ag@PEG/Apt (500 μg/mL, 60 μL) or PBS were intravenously injected into 4T1 tumor-bearing mice, respectively and then irradiated with 808 nm laser at a power density of 1 W/cm^2 for 5 min. For the comparision of photothermal signals in tumor and normal tissues, Au@Ag@PEG/Apt (500 μg/mL, 25 μL) and AuNS (500 μg/mL, 25 μL) were intratumorally or intramuscularly injected into tumor tissues and muscles, respectively and then laser irradiated for

10 min. Temperature changes of the tumor tissues and muscles were recorded by an IR thermal camera.

In Vivo Photothermal Therapy

4T1 tumor-bearing mice were randomly divided into five groups (n = 4 for each group): (I) PBS with laser irradiation, (II) Au@Ag@PEG without laser irradiation, (III) Au@Ag@PEG/Apt without laser irradiation, (IV) Au@Ag@PEG with laser irradiation, and (V) Au@Ag@PEG/Apt with laser irradiation. Laser irradiation (808 nm, 1 W/cm^2, 5 min) was performed after 12 h post-injection of indicated materials. Tumor volume and body weight of each mouse were recorded every other day for 14 days. After the whole therapeutic process, tumor and major organs (heart, liver, spleen, lung, and kidney) were collected for histological analysis.

Histological Analysis

The heart, liver, spleen, lung, kidney, and tumor from every group were resected and fixed with 4% formaldehyde for hematoxylin and eosin (H&E) and terminal deoxynucleotidyl transferase dUTP nick end labeling (TUNEL) assays.

Statistical Analysis

Data of experiment were represented as mean ± standard deviation (SD). Statistical analysis was conducted by one-way ANOVA with Bonferroni multiple comparisons post-test in Graphpad Prism 7.0. Significance was indicated as *P < 0.05, **P < 0.01 and ***P < 0.001.

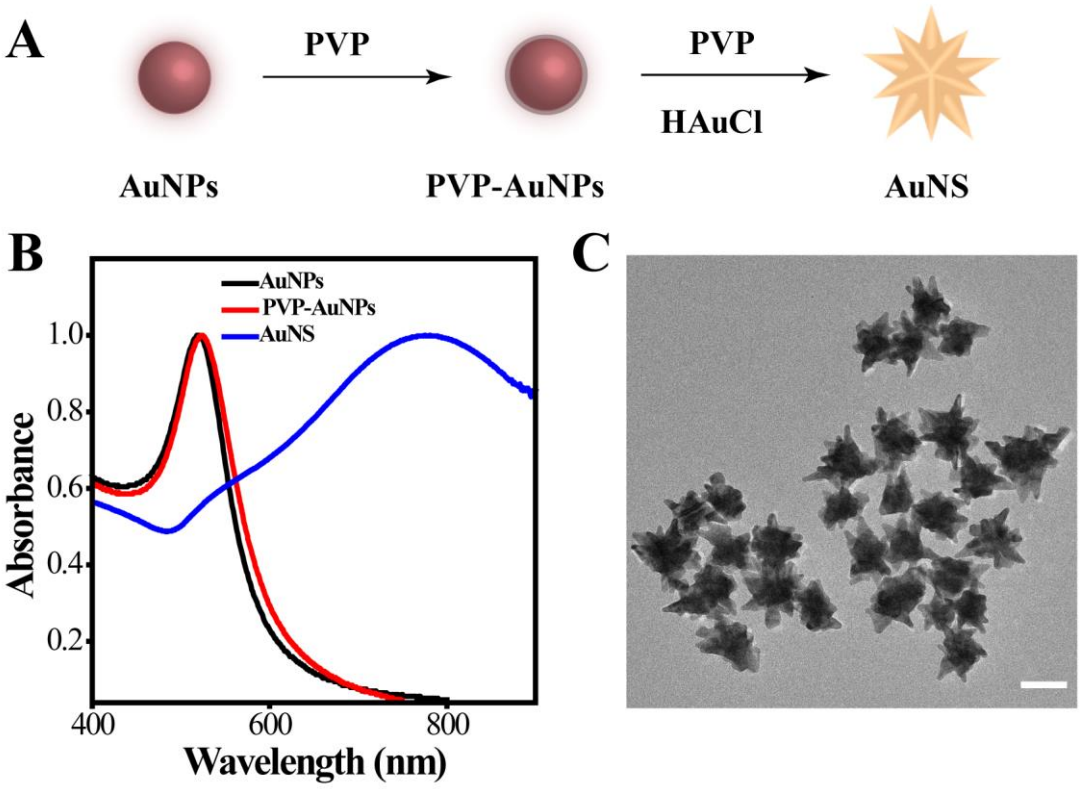

Figure S1. Preparation and characterization of AuNS. (A) Schematic illustration of the preparation of AuNS. (B) Normalized UV-vis absorption spectra of AuNPs, PVP-AuNPs, and AuNS. (C) TEM image of AuNS. Scale bar represents 50 nm.

Polyvinylpyrrolidone-modified gold nanoparticles (PVP-AuNPs) were prepared as the seed for the growth of AuNS.[1] Surface plasmon resonance peak of the AuNPs shifted from 519 to 523 nm after PVP modification, which was similar to our previous work.[2] AuNS displayed a broad plasmon peak at 775 nm with multiple sharp tips.

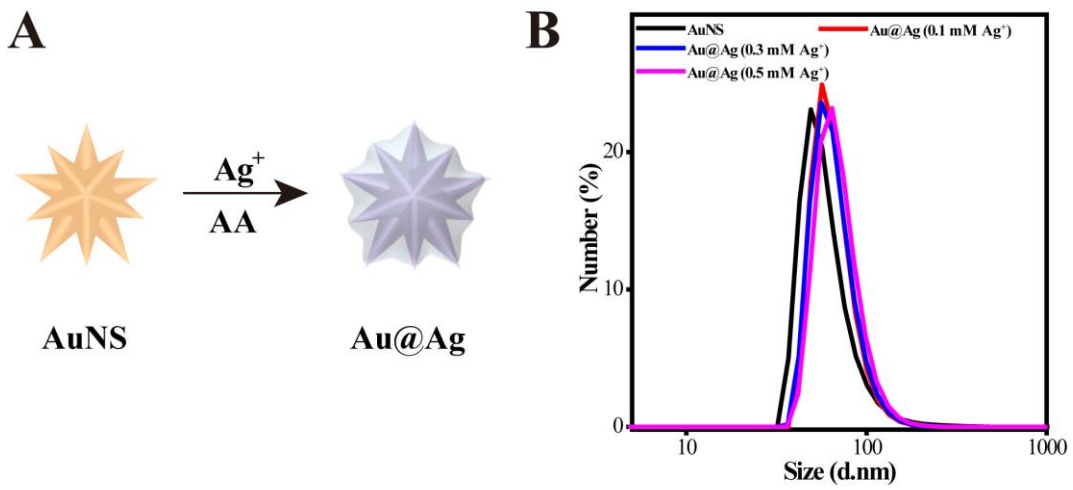

Figure S2. Preparation and characterization of Au@Ag nanostars. (A) Schematic illustration of the preparation of Au@Ag nanostars through silver coating on AuNS. (B) Variation in dynamic light scattering measurements of Au@Ag nanostars with different concentration Ag^+.

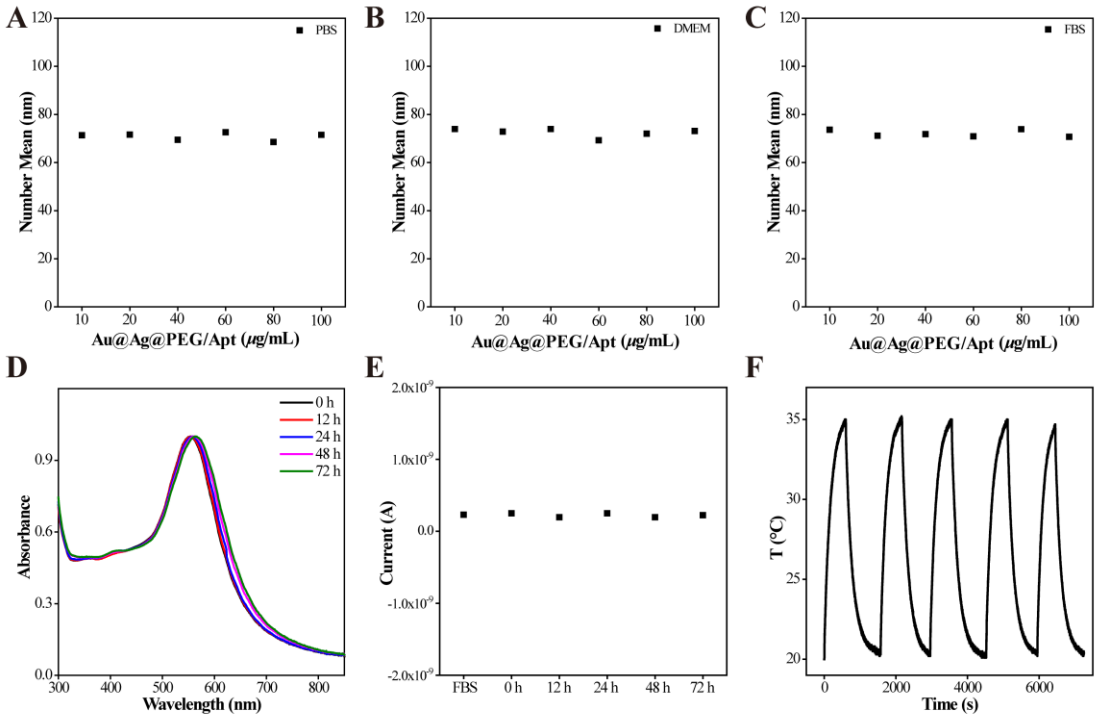

Figure S3. Stability of Au@Ag@PEG/Apt. Stability of Au@Ag@PEG/Apt in PBS (A), DMEM containing of 10% FBS (B), and FBS solution (C). (D) Normalized UV-vis absorption spectra of Au@Ag@PEG/Apt in FBS at different time. (E) Electrochemical signal change of Au@Ag@PEG/Apt supernatant solutions in (D). (F) Photostability of Au@Ag@PEG/Apt under laser irradiation. The laser wavelength was 808 nm with a power density of 1 W/cm^2.

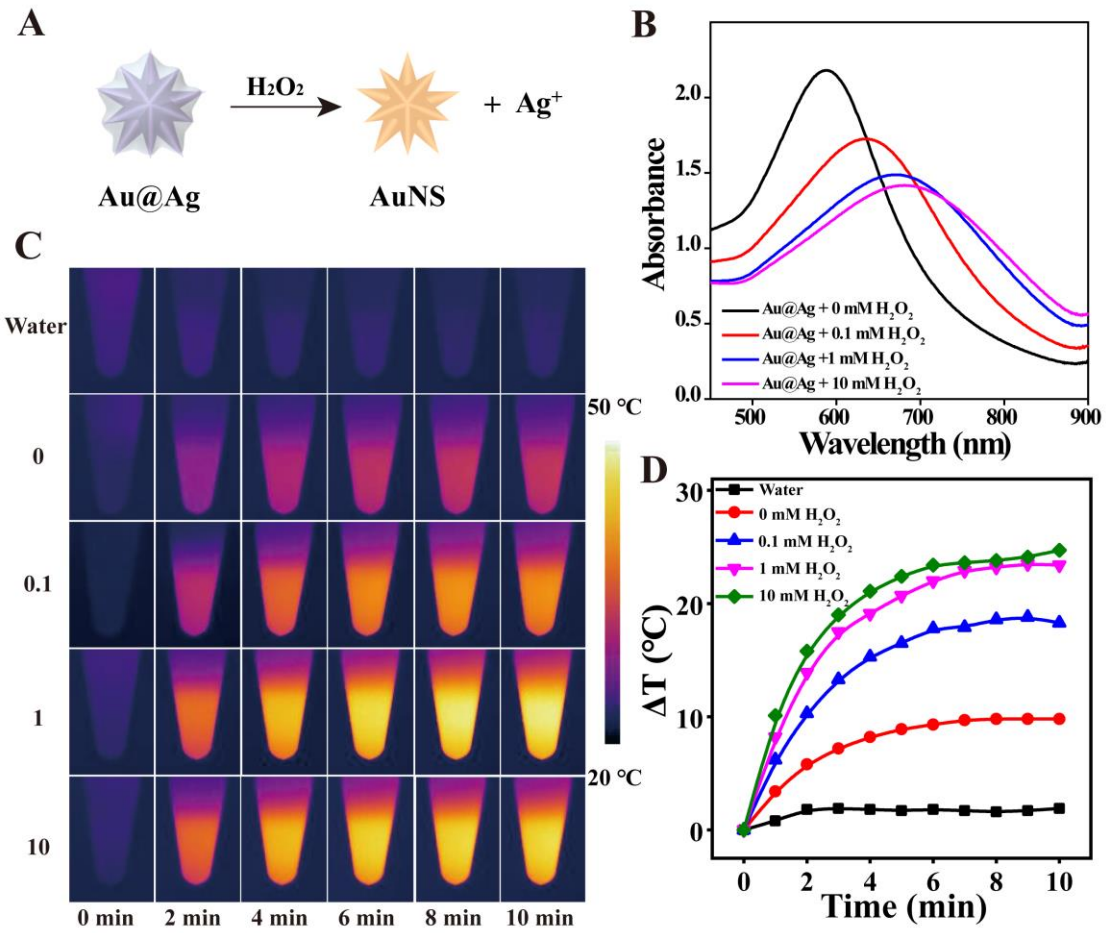

Figure S4. Changes in UV-vis absorption spectra and photothermal effect of Au@Ag nanostars after H_2O_2 activation. (A) Schematic illustration of Au@Ag nanostars etched by H_2O_2. (B) Changes in UV-vis absorption spectra, (C) infrared thermal images and (D) Time-dependent temperature change curves of the Au@Ag nanostars solution after respond to different concentrations of H_2O_2 (0, 0.1, 1, and 10 mM). The laser wavelength was 808 nm with a power density of 1 W/cm^2.

The data showed that the LSPR peak of Au@Ag nanostars gradually red-shifted and the NIR absorption enhanced prominently with increased H_2O_2 concentration. Moreover, the maximum temperatures of Au@Ag nanostars raised from 32.5 °C to 54.2 °C after adding H_2O_2, indicating an excellent H_2O_2 responsiveness of the dormant nanoparticles.

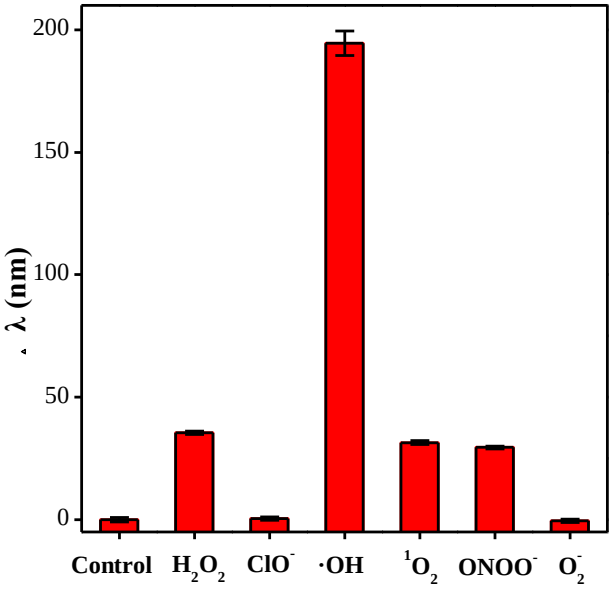

Figure S5. Red-shift of UV-vis absorption spectra of Au@Ag@PEG/Apt under various ROS. Concentration: 100 μM. Data are represented as mean ± SD (n=3)

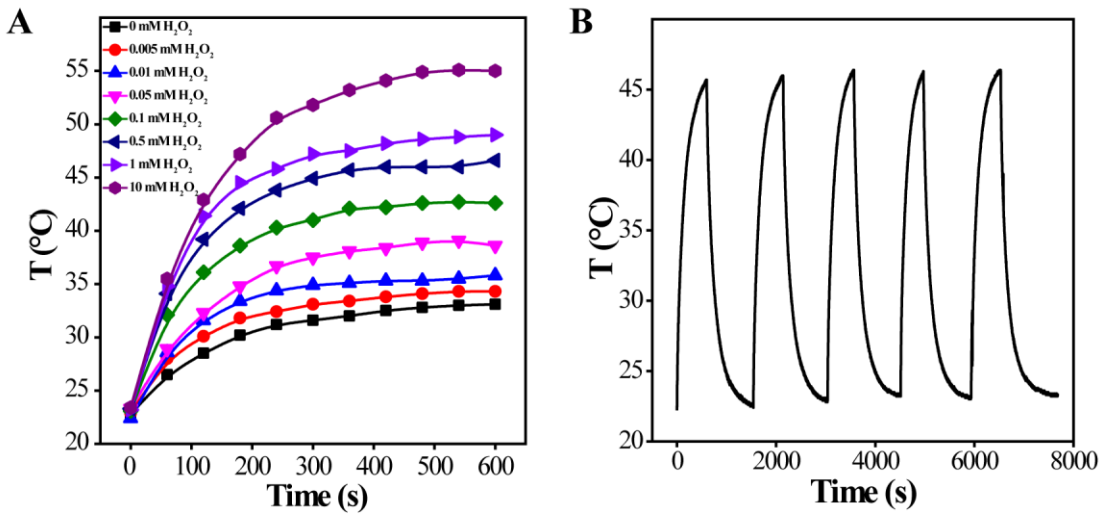

Figure S6. Photothermal effect of Au@Ag@PEG/Apt upon H_2O_2 stimulus. (A) Time-dependent temperature change curves of Au@Ag@PEG/Apt after H_2O_2 activation under NIR laser irradiation. (B) Photostability of Au@Ag@PEG/Apt with 100 μM H_2O_2 under laser irradiation. The laser wavelength was 808 nm with a power density of 1 W/cm^2.

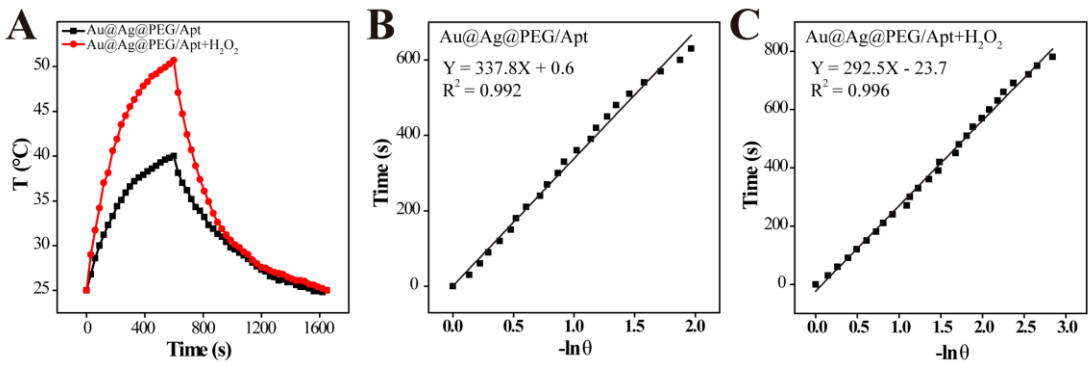

Figure S7. Determination of photothermal conversion efficiency (η) of Au@Ag@PEG/Apt. (A) Temperature changes of Au@Ag@PEG/Apt before and after H_2O_2 activation with 808 nm laser irradiation. The laser was shut off when temperature was stable. (B) Linear time data versus-ln θ obtained from the cooling period of Au@Ag@PEG/Apt before activation in (A). (C) Linear time data versus-ln θ obtained from the cooling period of Au@Ag@PEG/Apt after activation in (A).

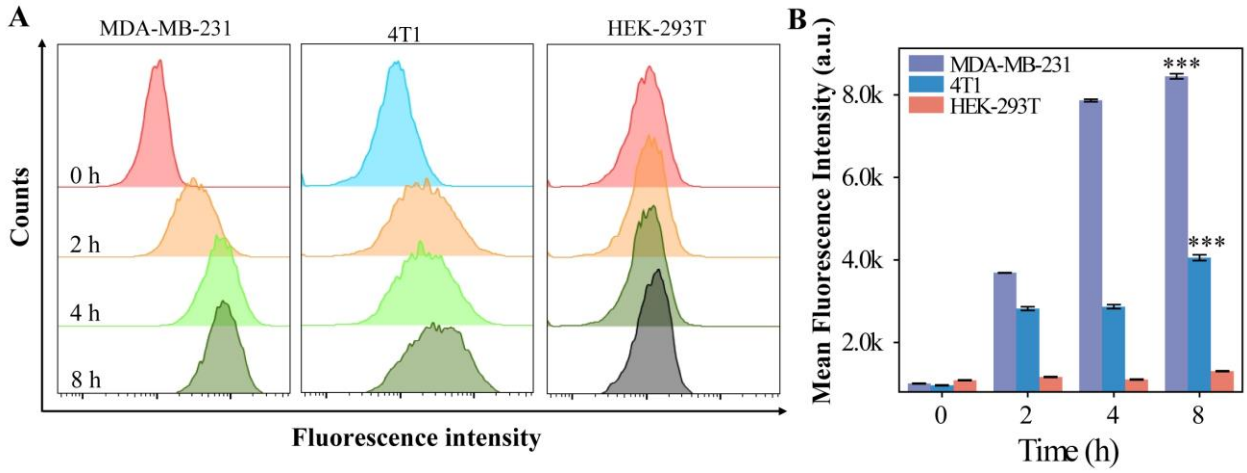

Figure S8. Flow cytometric analysis of different cells uptake of Au@Ag@PEG/Apt-TAMRA at different time points.

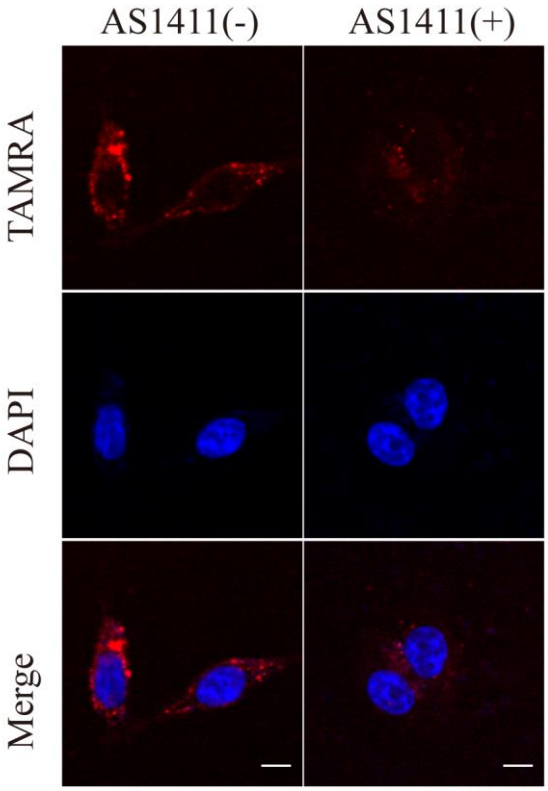

Figure S9. Fluorescence microscopy images of MDA-MB-231 cells pretreated with or without AS1411 upon Au@Ag@PEG/Apt-TAMRA incubation.

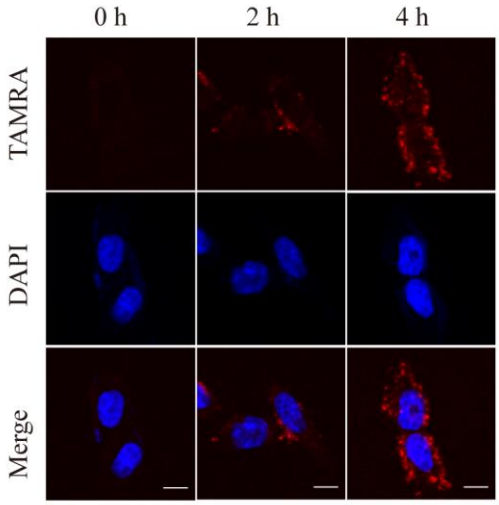

Figure S10. Fluorescence imaging of MDA-MB-231 cells after incubation with the nanoprobes for different time

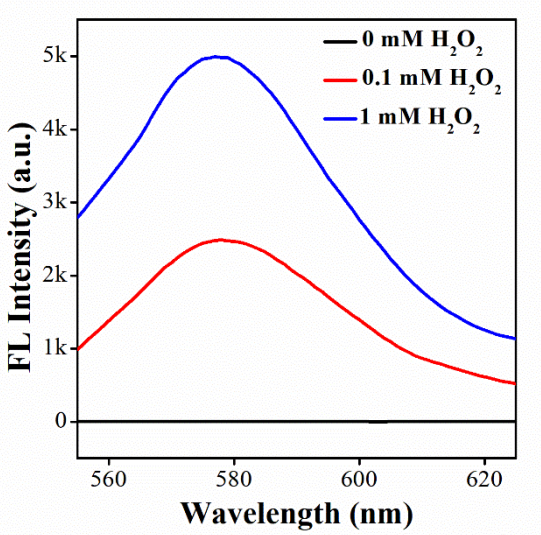

Figure S11. Fluoresence spectra of Au@Ag@PEG/Apt supernatant solutions in the absence or presence of H_2O_2.

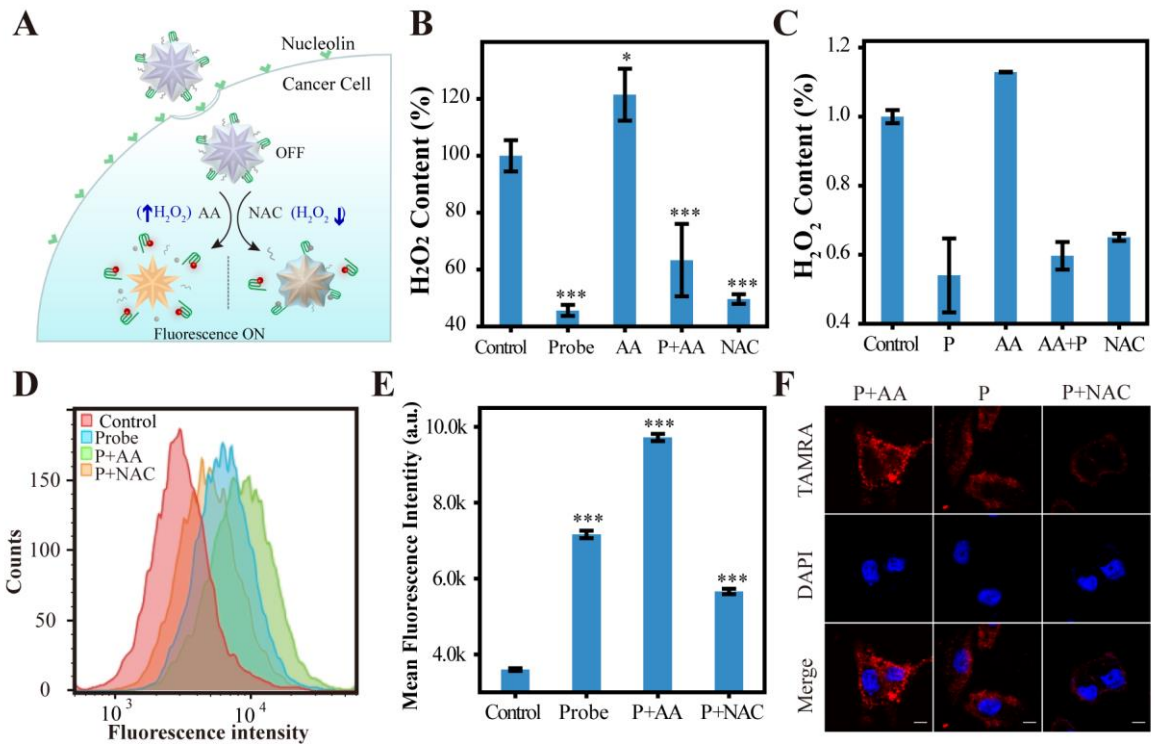

Figure S12. Tumor-specific nanoprobes allow fluorescence imaging of intracellular H_2O_2 dynamics. (A) Schematic illustration of the cancer cell specific and H_2O_2-activated fluorescence of Au@Ag@PEG/Apt-TAMRA. Upon Ag shell etching, previous quenched TAMRA is detached from the surface of the nanocrystals, activating the fluorescence of the fluorophore. Intracellular H_2O_2 levels were tuned using ascorbic acid (AA) as enhancer and N-Acetyl-L-Cysteine (NAC) as inhibitor. (B, C) Relative quantitation of H_2O_2 levels in MDA-MB-231 cells (B) and 4T1 cells (C). Cells were treated with PBS (control), Au@Ag@PEG/Apt (P), ascorbic acid (AA), ascorbic acid and Au@Ag@PEG/Apt (P+AA), and N-Acetyl-L-Cysteine (NAC). (D-F) Fluorescence analysis of intracellular H_2O_2 dynamics with flow cytometry (D, E) and confocal microscopy (F). The MDA-MB-231 cells were treated with the probe (P), probe plus AA (P+AA), and probe plus NAC (P+NAC). Scale bar, 10 μm. Statistical significance was calculated *via* one-way ANOVA with Bonferroni multiple comparisons post-test (*$P < 0.05$; ***$P < 0.001$); data are represented as mean ± SD ($n = 3$).

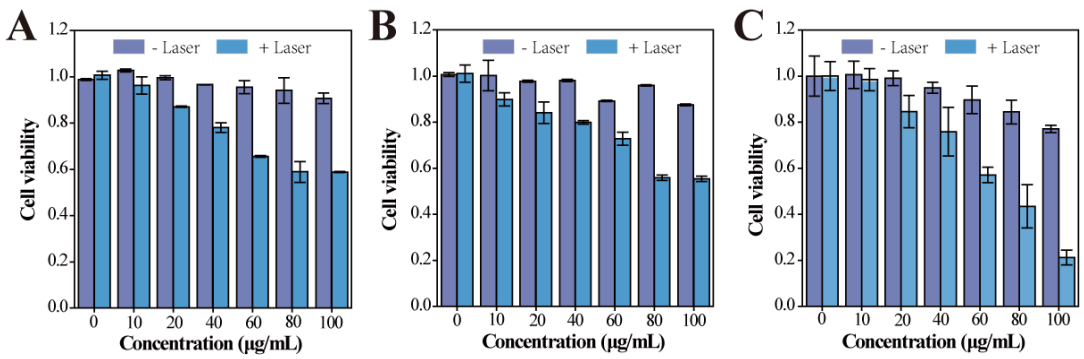

Figure S13. MTT experiments for Au@Ag@PEG and Au@Ag@PEG/Apt in the absence (purple) or presence (blue) of NIR laser irradiation. (A) Viability of MDA-MB-231 cells treated with Au@Ag@PEG nanostars. (B) Viability of 4T1 cells treated with Au@Ag@PEG. (C) Viability of 4T1 cells treated with Au@Ag@PEG/Apt. The laser wavelength was 808 nm with a power density of 1 W/cm^2. Data are represented as mean ± SD (n = 3)

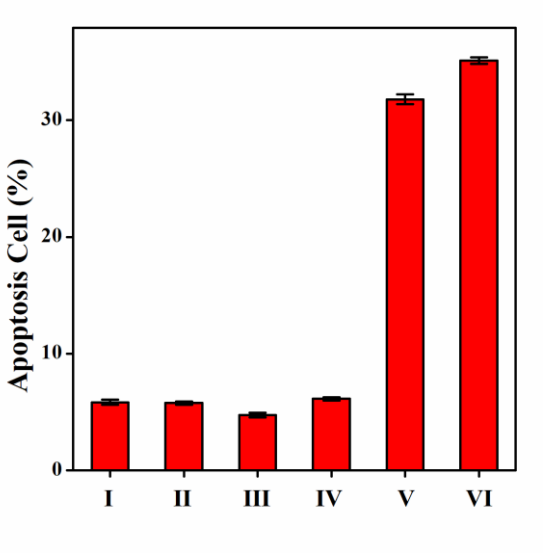

Figure S14. Statistical analysis of apoptosis cells (sum of annexin V-FITC$^+$/PI$^+$ and annexin V-FITC$^+$/PI$^-$) of MDA-MB-231 cells under different treatments: (I) PBS, (II) PBS plus laser irradiation, (III) Au@Ag@PEG, (IV) Au@Ag@PEG/Apt, (V) Au@Ag@PEG plus laser irradiation, and (VI) Au@Ag@PEG/Apt plus laser irradiation. The laser wavelength is 808 nm with a power density of 1 W/cm^2.

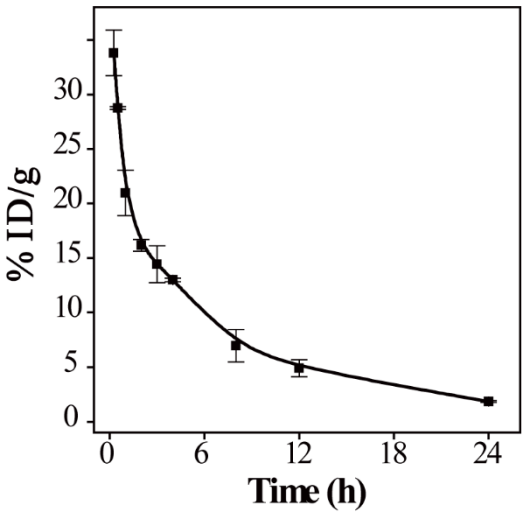

Figure S15. The blood clearance kinetics of Au@Ag@PEG/Apt after *i.v.* injection. Data are represented as mean ± SD (n = 3)

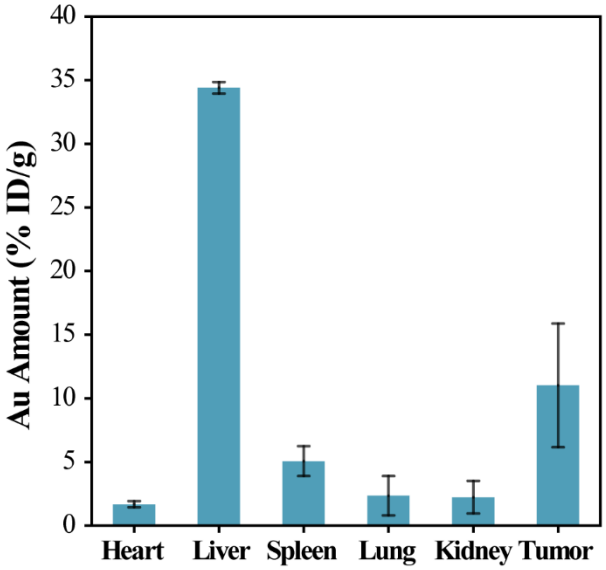

Figure S16. Biodistribution of Au amount in 4T1 tumor-bearing mice after 24 h post-intravenous injection of Au@Ag@PEG/Apt. Data are represented as mean ± SD (n = 3)

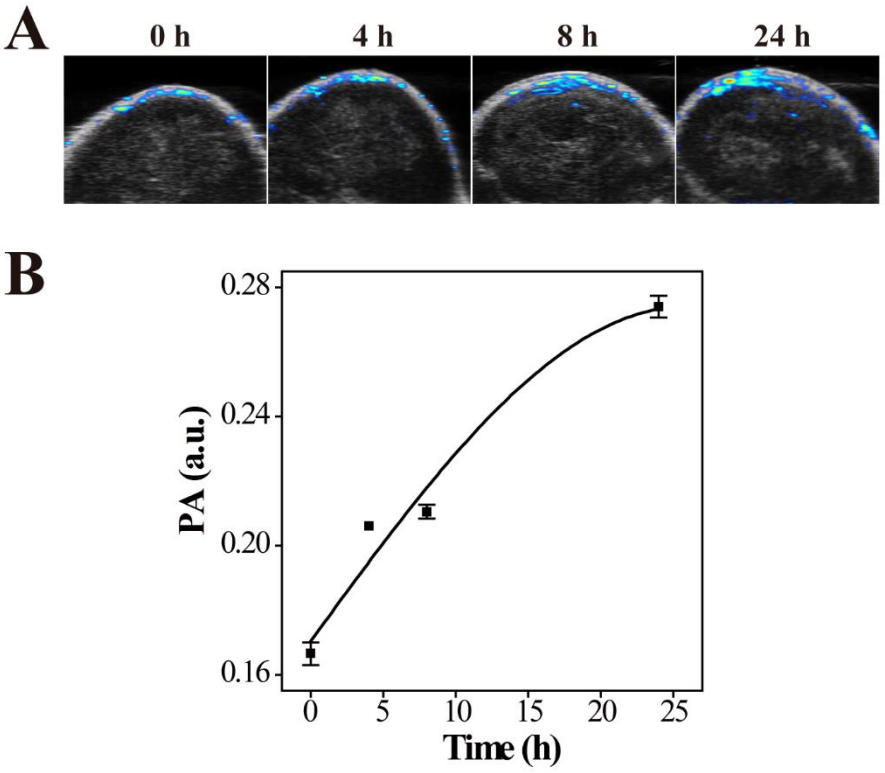

Figure S17. (A) PA images and (B) corresponding PA intensity of 4T1 tumor-bearing mice at different time points after *i.v.* injection with Au@Ag@PEG/Apt.

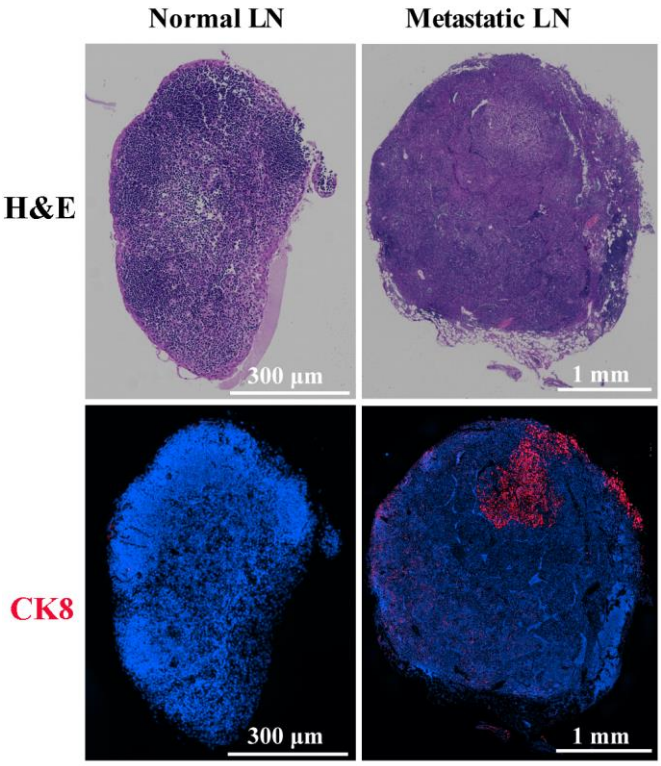

Figure S18. H&E and cytokeratin 8 (CK8) staining for metastatic lymph nodes and normal lymph nodes. Blue fluorescence: DAPI. Red fluorescence: CK8.

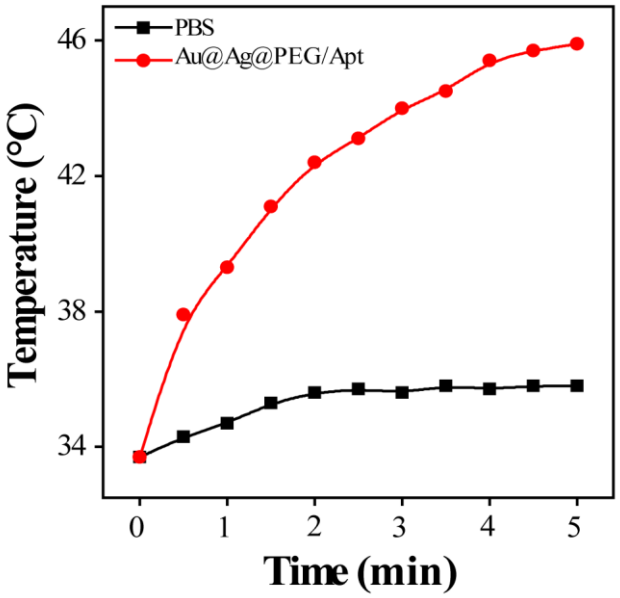

Figure S19. Time-dependent temperature change curves at tumor sites of 4T1-bearing mice treated with PBS and Au@Ag@PEG/Apt under laser irradiation. Laser wavelength, 808 nm, power density, 1 W/cm^2.

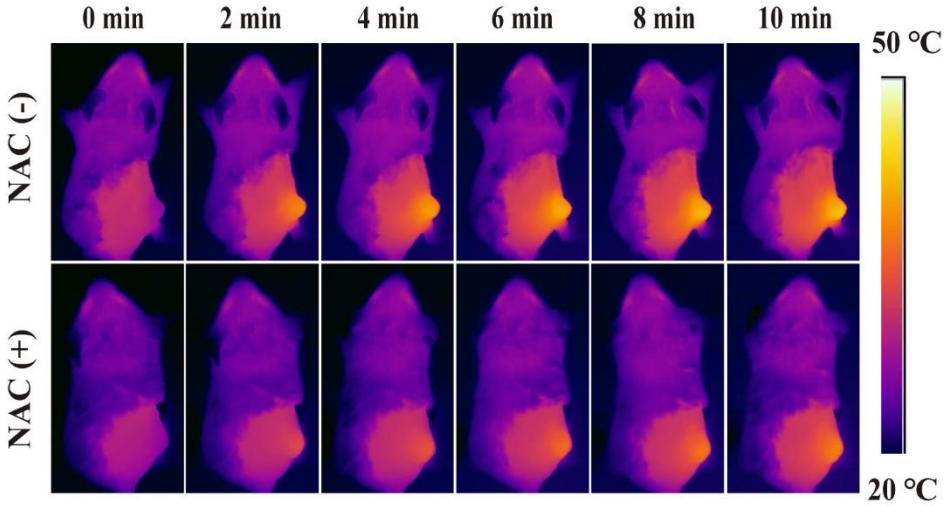

Figure S20. IRT images of 4T1 tumor-bearing mice after *i.t.* injection of Au@Ag@PEG/Apt, or Au@Ag@PEG/Apt with NAC pre-injection. The wavelength of the laser was 808 nm and the power density were 1 W/cm^2.

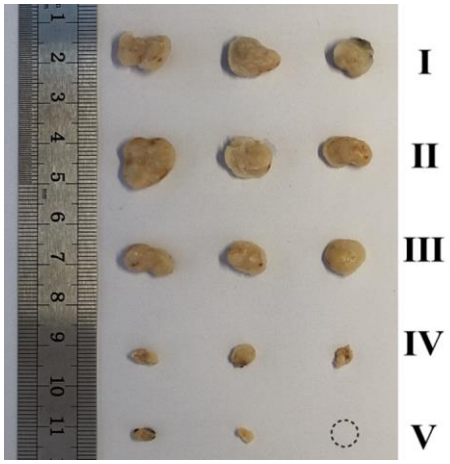

Figure S21. Photos of tumors extracted from mice after treatment for 14 days. (I) PBS+laser, (II) Au@Ag@PEG, (III) Au@Ag@PEG/Apt, (IV) Au@Ag@PEG+laser, (V) Au@Ag@PEG/Apt+laser. Laser wavelength, 808 nm; power density, 1 W/cm^2.

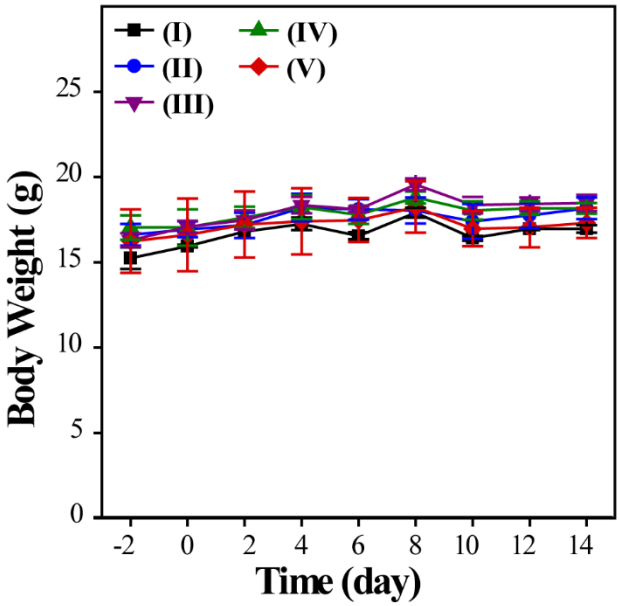

Figure S22. Changes of mice's body weight during treatment period. (**I**) PBS+laser, (**II**) Au@Ag@PEG, (**III**) Au@Ag@PEG/Apt, (**IV**) Au@Ag@PEG+laser, (**V**) Au@Ag@PEG/Apt+laser. Laser wavelength, 808 nm; power density, 1 W/cm^2. Data are represented as mean ± SD (n = 4)

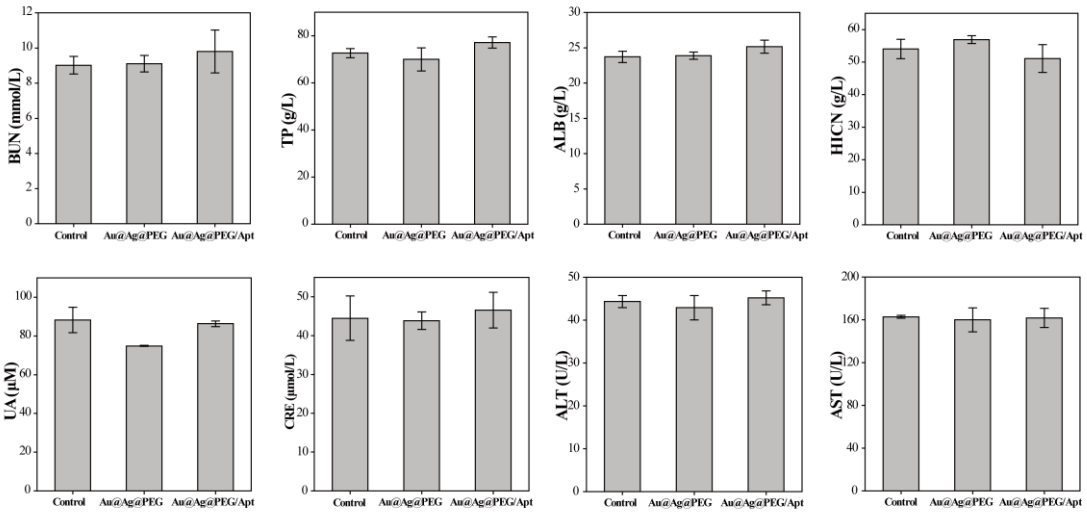

Figure S23. Serum biochemistry analysis of mice that were underwent with PBS, Au@Ag@PEG, and Au@Ag@PEG/Apt for 24 h (n = 3). The blood biochemical indexs include blood urea nitrogen (BUN), total protein (TP), albumin (ALB), hemiglobincyanide (HICN), uric acid (UA), creatinine (CRE), alanine aminotransferase (ALT), and aspartate aminotransferase (AST). Data are represented as mean ± SD (n = 3)

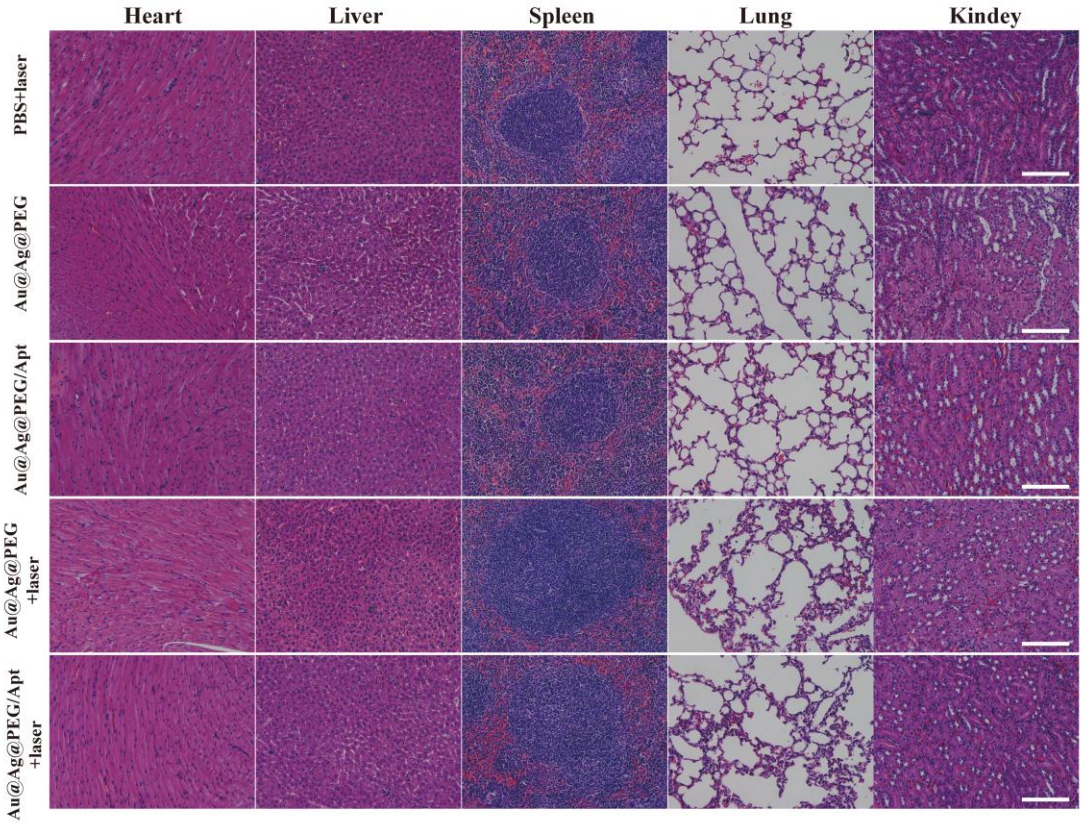

Figure S24. H&E staining images of the major organs collected from 4T1 tumor-bearing mice in the targeted treatment groups: PBS with laser irradiation (PBS+laser), Au@Ag@PEG, Au@Ag@PEG/Apt, Au@Ag@PEG with laser irradiation (Au@Ag@PEG+laser), and Au@Ag@PEG/Apt with laser irradiation (Au@Ag@PEG/Apt+laser).

Table S1. ICP-AAS analysis of Au@Ag@PEG/Apt.

Elements	Concentration (mg/L)	Molar ratio
Au	8.21	5.7:1
Ag	0.78	

References

1. P. Senthil Kumar, I. Pastoriza-Santos, B. Rodriguez-Gonzalez, F. Javier Garcia de Abajo, L. M. Liz-Marzan, *Nanotechnology*, 2008, **19**, 015606.

2. Y. Liu, M. Pan, W. Wang, Q. Jiang, F. Wang, D. W. Pang, X. Liu, *Anal. Chem.*, 2019, **91**, 2086-2092.

3. H. Kang, J. T. Buchman, R. S. Rodriguez, H. L. Ring, J. He, K. C. Bantz, C. L. Haynes, *Chem. Rev.*, 2018, **119**, 664-699.

4. B. Liu, J. Liu, *J. Am. Chem. Soc.*, 2017, **139**, 9471-9474.

5. B. Liu, T. Wu, Z. Huang, Y. Liu, J Liu, *Angew. Chem. Int. Ed.*, 2019, **58**, 2109-2113.